Northeast Siberian ice wedges confirm Arctic winter warming over the past two millennia

Article (Accepted Version)

Northeast Siberian ice wedges confirm Arctic winter warming over the past two millennia

Thomas Opel[1,2*], Thomas Laepple[1], Hanno Meyer[1], Alexander Yu. Dereviagin[3], Sebastian Wetterich[1]

[1] Alfred Wegener Institute, Helmholtz Centre for Polar and Marine Research, Periglacial Research Section, Telegrafenberg A43, 14473 Potsdam, Germany.

[2] now at University of Sussex, Department of Geography, Permafrost Laboratory, Brighton, BN1 9RH, United Kingdom

[3] Moscow State University, Department of Geocryology, Faculty of Geology, Vorob'evy Gory, 119899 Moscow, Russia.

[*] corresponding author: Thomas Opel (thomas.opel@awi.de, t.opel@sussex.ac.uk)

Abstract

Arctic climate has experienced major changes over the past millennia that are not fully understood in terms of their controls and seasonality. Stable-data from ice wedges in permafrost provide unique information on past winter climate. Recently, an ice-wedge record from the Lena River Delta suggested for the first time that Siberian winter temperatures increased throughout the Holocene, contradicting most other Arctic

paleoclimate reconstructions which are likely biased towards the summer. However, the representativeness of this single record and the spatial extent of its reconstructed winter warming signal is unclear. Here, we present a new winter temperature record based on paired stable oxygen ($\delta^{18}O$) and radiocarbon age data spanning the last two millennia from the Oyogos Yar coast in northeast Siberia. The record confirms the long-term winter warming signal as well as the unprecedented temperature rise in recent decades. This confirmation demonstrates that winter warming over the last millennia is a coherent feature in the northeastern Siberian Arctic, supporting the hypothesis of an insolation-driven seasonal Holocene temperature evolution followed by a strong warming likely related to anthropogenic forcing.

Keywords: Ice wedges, stable water isotopes, permafrost, Siberian Arctic, winter climate reconstruction, Late Holocene, Arctic2k

Introduction

Currently, the Arctic climate faces significant changes, expressed by a rapid warming that is more pronounced than in other regions of the Earth (Serreze and Barry, 2011; PAGES 2k Consortium, 2013). A sharp decrease in sea-ice area and thickness, enhanced melting of glaciers and ice caps, as well as warming and thawing of permafrost illustrate the vulnerability of the Arctic under recent conditions and in

particular for a predicted future warming (AMAP, 2011). Due to its importance for the global climate system, the Arctic is a key region to study past and recent climate variability and their environmental implications on different spatial, temporal and seasonal scales.

The Russian Arctic is underrepresented in Arctic paleoclimate records (Kaufman et al., 2009; PAGES 2k Consortium, 2013; McKay and Kaufman, 2014). Most records in the recent PAGES Arctic2k (McKay and Kaufman, 2014) and Arctic Holocene Transitions (Sundqvist et al., 2014) databases are based on biological proxies such as pollen and tree rings, which mainly record summer climate conditions. Hence, the reconstructions are either restricted or biased to summer conditions (Liu et al., 2014). But winter conditions, as obtained from ice wedges, are essential for a comprehensive assessment of past climate.

Ice wedges are widespread in permafrost regions and form by thermal contraction cracking in winter and filling of cracks by snow-melt water in spring (Lachenbruch, 1962). Due to this seasonality of cracking and filling, the contribution of summer precipitation can be excluded when analysing ice-wedge ice. Ice wedges can be studied using stable water isotopes (Mackay, 1983; Vaikmäe, 1989). As the meltwater in the frost crack refreezes rapidly, the isotopic signature of each resultant ice vein is directly related to atmospheric precipitation, i.e. snowfall in winter and spring, before snowmelt. Therefore, ice-wedge stable isotopes represent the climate conditions during the cold

period of a year from December to May (Meyer et al., 2015), hereafter referred to as winter.

Stable-isotope data from ice wedges have been used to reconstruct past climate in Siberian Arctic permafrost regions on glacial-interglacial timescales (e.g. Meyer et al., 2002a; Meyer et al., 2002b; Vasil'chuk and Vasil'chuk, 2014; Wetterich et al., 2011; Wetterich et al., 2014; Wetterich et al., 2016), as well as centennial timescales for the Lateglacial (Meyer et al., 2010) and the Holocene (Meyer et al., 2015). Meyer et al. (2015) suggested a Mid to Late Holocene winter warming trend based on stable-isotope studies of ice wedges in the Russian Arctic Lena River Delta (Figure 1), a remarkable finding given that the majority of paleoclimate records show a cooling trend.

To test whether the findings of Meyer et al. (2015) are also valid in a larger region and to test them with independent data, we present a new oxygen-isotope record from ice wedges at the Oyogos Yar coast in the northeast Siberian Arctic, about 570km east of the central Lena River Delta (Figure 1) (Opel et al., 2011). Our record is based on newly available radiocarbon ages of organic matter enclosed in ice-wedge samples used to generate a stacked record based on paired isotope and age information.

Study region

Oyogos Yar is on the southern coast of the Dmitry Laptev Strait in the permafrost lowlands of the northeast (Figure 1). The study site (72.7°N, 143.5°E) is located in a

vast thermokarst basin that formed due to permafrost degradation of Late Pleistocene Yedoma Ice Complex sequences (Schirrmeister et al., 2011; Opel et al., 2017) during the Lateglacial to Holocene transition (Wetterich et al., 2009). The Oyogos Yar coast is subject to rapid coastal erosion (-6.5 ± 0.2 m a^{-1}) (Günther et al., 2013) that leads to the development of steep coastal bluffs about 10 to 12 m high in the drained thermokarst basins (Figure 1). The thawed and refrozen Yedoma Ice Complex sediments are overlain by 1-2 m of lacustrine deposits that accumulated before the drainage of the former thermokarst lakes. The lacustrine deposits are covered by a distinctive peat horizon ca. 2 to 3 m below the surface and dating to 8 to 9 ky BP (Wetterich et al., 2009). In the Late Holocene, palustrine polygonal deposits have capped the sequence and contain syngenetic ice wedges (Opel et al., 2011).

[insert Figure 1]

Material and Methods

Fieldwork

Sampling took place after surveying coastal bluffs (Opel et al., 2011) to identify suitable Late Holocene ice wedges. We cut by chain saw complete horizontal profiles at depths of 1 to 1.5 m below surface in high sampling resolution (2-3 cm) along the growth direction of two ice wedges (Oy7-04 IW2 and Oy7-11 IW1). The samples were melted

on site and packed for further analysis. A complete horizontal profile of a third ice wedge (Oy7-11 IW7) was cut in blocks that were transported frozen to the cold laboratory for sub-sampling at low (4-6 cm) and high (1 cm) resolution. All three ice wedges were sampled less than 1 km apart. Additionally, we sampled ice veins from recently growing ice wedges (RIW) connected to the modern polygonal surface to capture reference records of modern wedge ice.

Stable water isotopes

To determine the stable-isotope composition, we used a Finnigan-MAT Delta S mass spectrometer with an analytical precision of better than ±0.1‰ for $\delta^{18}O$ and ±0.8‰ for δD, respectively (Meyer et al., 2000). The $\delta^{18}O$ and δD values of wedge ice are interpreted as proxies for local winter air temperatures (Meyer et al., 2015). The d excess ($d=\delta D-8\delta^{18}O$) (Dansgaard, 1964) indicates the evaporation conditions in the moisture source region (Merlivat and Jouzel, 1979). However, the involvement of other factors (atmospheric transport, moisture source changes, seasonality effects of frost cracking and snow-cover development) has to be considered. In our analysis we focus on stable oxygen isotopes ($\delta^{18}O$), which are commonly used in Arctic paleoclimate studies and therefore comparable to our record.

Radiocarbon dating and stacking procedure

To anchor the stable-isotope information in time, organic remains enclosed in 19 ice-wedge samples were radiocarbon-dated using the accelerator mass spectrometry (AMS) facilities at the Leibniz Laboratory (Kiel University, Germany) (Grootes et al., 2004) and CologneAMS (University of Cologne, Germany) (Dewald et al., 2013; Rethemeyer et al., 2013). Conventional ^{14}C ages were calculated according to (Stuiver and Polach, 1977) and were calibrated using the tool *clam* (Blaauw, 2010) with the IntCal13 dataset (Reimer et al., 2013). We report the highest posterior density region (hpd) with its limits, its midpoint and probability (Table 1). All hpd ranges add up to 95%. One post-bomb age was determined using the tool CALIbomb (Reimer et al., 2004) with $F^{14}C=1.2661\pm0.005$ and post-bomb calibration dataset NHZ1.

The age-model construction and stacking procedure follows Meyer et al. (2015). As every ice-wedge sample is dated with a separate ^{14}C measurement and the chronological order between single ice wedges is not determined by their position, age models were constructed by repeated sampling of point estimates from the calibrated distributions of the ages. To account for the effect of the age uncertainty on the proxy time series, 10,000 age models were constructed. For every age model a proxy curve was estimated by linearly interpolating the $\delta^{18}O$ values between the observed points. Finally, the 50, 90 and 99% quantiles of the $\delta^{18}O$ distribution for every point in time were calculated and plotted.

Climate model simulations

We analysed the monthly surface air temperature fields of seven simulations from five coupled climate models (CCSM4, IPSL-CM5A-LR, MPI-ESM-P, BCC-CSM1-1, GISS-E2-R) participating in the millennium simulations (past1000) of the third Palaeoclimate and the fifth Coupled Modelling Intercomparison Projects (PMIP3: Braconnot et al., 2012; CMIP5: Taylor et al., 2012). The MIROC simulation was omitted because of an unphysical drift over the simulated period.

We analysed the winter season, which we expect to be recorded in the ice wedges (DJFMAM), as well as the classical summer season (JJA) to represent the summer-biased proxies. We analysed the simulations for the study area (72-73N, 126-144E) and show the multi-model ensemble mean. Time series covering the years 850 to 2005 were constructed by appending the 20C3M simulations to the hist1000 simulations. We corrected for potential offsets between both simulations by aligning the mean of the last years of the hist1000 simulation (1844-1849) with the mean of the first years of the 20C3M simulations (1850-1854).

Results

Ice-wedge stable-isotope data

We analyzed 485 samples from the three ice wedges; 107 samples from Oy7-04 IW2, 123 from Oy7-11 IW1, 210 from Oy7-11 IW7 (high-resolution profile) and 45 from

Oy7-11 IW7 (low-resolution profile). Additionally, 14 samples from eight RIW were analyzed to represent the most recent ice-wedge rejuvenation stages, i.e. modern ice-wedge growth. Near the profile margins, isotopic exchange with enclosing sediments (Meyer et al., 2002a) can alter the isotopic composition. We therefore omitted 26 samples from the profile margins that show distinct signs of isotopic alteration, i.e. strongly increased $\delta^{18}O$ (Figure 2) and decreased d excess values, from the further analysis.

The three ice-wedge $\delta^{18}O$ datasets show similar statistical properties independent of ice-wedge width or sampling resolution (Figure 2). The minimum $\delta^{18}O$ values per ice wedge vary between -27.1 and -26.5‰, the maximum values between -21.6 and -20.7‰ and mean values between -25.1 and -25.0‰. The regression in $\delta^{18}O$-δD co-isotopic plots reveal slopes between 7.6 and 7.7, with intercepts between -2.2 and -0.8 and R^2 values of 0.99 for each profile. The RIW $\delta^{18}O$ data vary between -24.4 and -18.2‰. The mean value of -20.7‰ equals the maximum value of ice wedge Oy7-11 IW7. The co-isotopic regression slope is 7.8 and the intercept 3.2 (R^2=0.99). The isotopic compositions of Late Holocene and recent ice wedges plot close to the GMWL (Global Meteoric Water Line: $\delta D=8\delta^{18}O+10$) (Craig, 1961), which suggests that major secondary isotope fractionation effects can be neglected.

A common feature of all $\delta^{18}O$ profiles is the predominance of low values (-27 to -25‰) in the outer parts of the profiles, i.e. the older ice-wedge sections (Figure 2). In contrast,

the younger sections in the central parts of the profiles (except for Oy7-11-IW1), exhibit generally higher values $\delta^{18}O$ values (above -24‰). The low-resolution profile of ice wedge Oy7-11- IW7 closely resembles the corresponding high-resolution profile (R=0.98, after bringing both to the same resolution). The $\delta^{18}O$ maxima of the profiles (-21.6 to -20.7‰) correspond to the $\delta^{18}O$ values of the respective RIW $\delta^{18}O$ values (Figure 2) and are relate directly to (i.e. underlie) the recent ice-wedge rejuvenation stages (Figure 5 in Opel et al., 2011).

The ice wedges Oy7-04-IW2 and, in particular, Oy7-11-IW7 show symmetric $\delta^{18}O$ profiles with the highest $\delta^{18}O$ values and modern ages in the central ice-wedge part as mirror axes (Figure 2). In contrast, ice wedge Oy7-11 IW1 lacks symmetry, indicating peripheral ice-wedge development rather than central frost cracking and growth.

[insert figure 2]

Radiocarbon dating

Radiocarbon ages cluster in two distinct groups: 14 out of 19 ages are from the last two kyr BP, whereas five ages range from 3.5 to 14 kyr BP (Table 1). The latter ages, which we now discuss in detail, likely represent older reworked organic material and are, therefore, excluded from chronology interpretation. The age of sample Oy7-11-Hy31 corresponds to the initiation of the lacustrine phase in the thermokarst basin. Sample

Oy7-04-247 contained only degraded organic material with very low carbon content (Opel et al., 2011). The ages of the peaty material in samples Oy7-11-138, Oy7-11-162 and sample Oy7-11-Hy40 fit well to that of the distinctive peat layer (Wetterich et al., 2009) about 1 to 1.5 m below the sampling depth and may therefore originate from this horizon (Opel et al., 2011). Relocation of older material may be caused by the upward bending of sediment layers close to the ice wedges (Figure 1).

Generally, younger ages are related to the central ice-wedge parts with higher $\delta^{18}O$ values, whereas the outer parts show older ages (Figure 2). Except for one age each in both symmetric profiles, all radiocarbon ages are in "logical chronological order" as implied by the schematic (i.e. central) ice-wedge growth model (Lachenbruch, 1962).

Stacked $\delta^{18}O$ record

We used the paired $\delta^{18}O$ and calibrated radiocarbon age information of the 14 ice-wedge samples from all three ice wedges to generate a stacked $\delta^{18}O$ record. We additionally added the mean $\delta^{18}O$ value of RIW, related to the period AD2000-2007 that represents the most recent data point. The stacked $\delta^{18}O$ record spans roughly two millennia. It exhibits a general increase in $\delta^{18}O$ of about 1.5‰ per 1,000 years, with an unprecedented maximum obtained in the most recent samples (Figure 3).

Discussion

Oyogos Yar ice-wedge $\delta^{18}O$ based climate reconstruction

The predominance of ages younger than 2,000 years shows increased horizontal growth activity of the studied ice wedges at the height of the sampled profiles. This suggests relatively stable polygonal surface conditions in the thermokarst basin over the last two millennia, without substantial sediment accumulation and corresponding vertical ice-wedge growth. Such stability is in line with field observations of ice-wedge shapes (Figure 1). It also indicates that the horizontal ice-wedge $\delta^{18}O$ profiles are not significantly influenced by vertical ice-wedge growth and, therefore, are suitable for paleoclimatic interpretation. Their suitability is supported by the mean ice-wedge isotopic compositions close to the GMWL, indicating the preservation of climate signals in ice-wedge stable isotopes. In the following, we attribute the $\delta^{18}O$ evolution recorded by the ice wedges to winter temperature changes as the stable isotope composition of Arctic precipitation depends mainly on local air temperatures (Meyer et al., 2015).

[insert Figure 3]

The stacked Oyogos Yar $\delta^{18}O$ record shows a warming trend (Figure 3). This trend is also confirmed in each of the three ice-wedge $\delta^{18}O$ profiles (Figure 2), emphasizing, that this millennial warming is not an artefact of stacking.

The warming culminates in an unprecedented recent $\delta^{18}O$ maximum attributed to the Arctic amplification of climate change. This recent $\delta^{18}O$ maximum might be slightly amplified by substantial changes in the Arctic climate system. Slight changes in the seasonal distribution of precipitation may increase the contribution of isotopically heavier early and/or late winter precipitation to the total snowpack. Additionally, ongoing warming and associated decline of sea-ice extent and later freeze-up in the Russian Arctic may affect the $\delta^{18}O$-temperature relationship. Modelling results suggest that higher temperatures and lower sea-ice extent enhance local to regional evaporation (Faber et al., 2016). An increase of locally-derived moisture that is less depleted than water vapour transported over long distances may increase the $\delta^{18}O$ values of precipitation. However, even though these processes may adapt the long-term $\delta^{18}O$-temperature relation to recent Arctic climate change, they support the paleoclimatic interpretation of our $\delta^{18}O$ stack.

The Oyogos Yar $\delta^{18}O$ stack shows a similar evolution as that of the Lena River Delta $\delta^{18}O$ stack (Meyer et al., 2015), (Figure 3). Both reconstructions are significantly correlated to each other ($R=0.52$, $p=0.01$ accounting for autocorrelation and the interpolation before correlation), which is mainly due to the simultaneous strong increase of $\delta^{18}O$ values in the last century. Both stacked ice-wedge records reveal that highest $\delta^{18}O$ values of the Late Holocene correspond to radiocarbon-dated samples of post-bomb origin as well as actively growing recent ice wedges.

However, the isotopic increase during the last centuries in the Oyogos Yar stack (3.5‰ increase between the mean $\delta^{18}O$ before and after AD1800) is more pronounced than that in the Lena River Delta record (2.4‰). Interestingly, both the preindustrial (before AD1800) variability as well as this recent warming are amplified by a similar amount. The ratio of preindustrial standard deviations is 1.6 (Oyogos Yar: 1.1‰; Lena River Delta: 0.7‰), and the ratio of the recent warming amplitude is 1.5.

The ice wedges that form the Oyogos Yar stack were studied less than 1 km apart, while the ice wedges that form Lena River Delta stack originate from a larger sampling area. Therefore, the higher Oyogos Yar variability is unlikely to be an artefact of mixing spatial and temporal variability but instead relates to a stronger climate variability in this region. This might be explained by its more northeasterly location and corresponding feedback effects, such as sea ice and polynya variability, that likely differ from the central Lena River Delta.

The multi-model mean of the CMIP5 climate model simulations (Figure 3) shows a slight decrease in temperature until ~1750, followed by a warming for both winter (DJFMAM) and summer (JJA). This simulated winter cooling trend (-0.54K / kyr) likely relates to a combination of nonlinear responses to insolation, as well as increased volcanic forcing (PAGES 2k Consortium, 2013). The cooling trend is within the uncertainty of the Oyogos Yar ice-wedge trend estimate (850-1750, 0.3±1.8 (1se) K/kyr), demonstrating that the ice-wedge record is too coarse to infer whether the model

overestimates the cooling trend. Interestingly, the model simulations clearly suggest that the Arctic winter warming in the last century is much stronger than changes in the annual mean (not shown) or summer (Screen et al., 2010). This is consistent with the strong warming observed in both ice-wedge records, and it explains why Siberian ice wedges as particular winter climate archives, despite their associated uncertainties, record the unprecedented warming.

Implications for Late Holocene Arctic paleoclimatology

To our knowledge the Oyogos Yar and Lena River Delta ice-wedge records represent the only available Late Holocene ice-wedge records that are dated to sub-millennial scale. Their similarity shows that the reconstructed winter warming trends are at least representative for the northeast Siberian Arctic. Case studies on Svalbard and the Yamal Peninsula (Vasil'chuk et al., 2015) as well as a review on ice-wedge isotopes across the Russian Arctic (Streletskaya et al., 2015) lack well-constrained geochronological information based on sufficient radiocarbon data of ice-wedge samples and are therefore of limited use for centennial- to millennial-scale paleoclimate reconstruction.

It is noteworthy that the nearest millennial record based on tree-ring width from Avam-Taimyr (Briffa et al., 2008), interpreted as June-July temperatures, lacks any long-term trend over the last two millennia. Shorter regional, i.e. northeast Siberian, tree-ring records from the Lower Lena River (MacDonald et al., 1998) and Indigirka (Hughes et

al., 1999), interpreted as June and early summer temperatures, respectively, show warming trends over the past six centuries. However, interpreting long-term climate trends from tree-ring records is challenging (Cook et al., 1995). The nearest ice-core $\delta^{18}O$ record to our study area, from Severnaya Zemlya (Opel et al., 2013), has been interpreted as a proxy for annual mean temperatures and does not show any long-term trend over the past millennium. However, these tree-ring and ice-core records show a cooling trend up to AD1850 due to the Late Holocene decreasing summer insolation. This is expected since all these reconstructions are biased towards summer. The pronounced warming they exhibit after AD1850 underlines the extent of the recent Arctic amplification to global warming.

The reconstructed ice-wedge winter warming trend over the past two millennia clearly contradicts most other Arctic proxy records and compilations (Kaufman et al., 2009; PAGES 2k Consortium, 2013; McKay and Kaufman, 2014) (Figure 3). This likely relates to the climate response on the seasonally differing insolation forcing (Laskar et al., 2004). For winter (November to April, NDJFMA), insolation at 60°N has slightly increased, whereas for summer (May to October, MJJASO) it has decreased (Figure 3). Additionally, increasing atmospheric greenhouse gas concentrations (Joos and Spahni, 2008) (Figure 3) may have contributed to the long-term warming already before and especially during industrial times. As pointed out by several studies, non-linear internal feedbacks from ocean, sea-ice and land-cover changes have an additional impact on the

Arctic temperature evolution, in particular during winter (Braconnot et al., 2007; Zhang et al., 2010). Here, our winter $\delta^{18}O$ stack, in combination with isotope-enabled climate models (Werner et al., 2011), might help to elucidate the strength of these feedback processes.

Conclusions and outlook

Our presented data highlight the potential of ice wedges in permafrost as promising and unique archives of winter climate. This is particularly important for the Holocene, when summers and winters show opposite insolation trends. The stacked Oyogos Yar ice-wedge $\delta^{18}O$ record shows a long-term winter warming over the last two millennia, with an unprecedented recent maximum. It independently confirms the results of Meyer et al. (2015). Our results imply that, the seasonality of climate archives and proxies needs to be better constrained before comparing proxy records with climate model results, in particular for the Arctic. Ultimately, a better understanding of the relationship of climate variations, variations in $\delta^{18}O$ of the precipitation and the signal preserved in the ice wedges is needed to better quantify the reconstruction of past temperatures. More ice-wedge studies are essential as well as new approaches for ice-wedge chronologies to increase the temporal resolution of ice-wedge-based climate reconstructions.

Acknowledgements

The study presented here is part of the Russian-German System Laptev Sea cooperative scientific effort. We thank our colleagues who helped during fieldwork and following discussions as well as the staff from the AWI Potsdam stable isotope laboratory. This study contributes to the ‘Eurasian Arctic Ice 4k’ project (Deutsche Forschungsgemeinschaft grant no. OP217/2-1) and was supported by the Initiative and Networking Fund of the Helmholtz Association Grant VG-NH900. The Program for Climate Model Diagnosis and Intercomparison and the World Climate Research Programme Working Group on Coupled Modeling made the WCRP CMIP5 simulations available. We thank two anonymous reviewers and Julian Murton for their comments that helped us to improve the manuscript.

References

AMAP. (2011) Snow, Water, Ice and Permafrost in the Arctic (SWIPA): Climate Change and the Cryosphere. Oslo, Norway, xii + 538 pp.

Blaauw M. (2010) Methods and code for 'classical' age-modelling of radiocarbon sequences. *Quaternary Geochronology* 5: 512-518.

Braconnot P, Otto-Bliesner B, Harrison S, et al. (2007) Results of PMIP2 coupled simulations of the Mid-Holocene and Last Glacial Maximum - Part 1: experiments and large-scale features. *Climate of the Past* 3: 261-277.

Braconnot P, Harrison SP, Kageyama M, et al. (2012) Evaluation of climate models using palaeoclimatic data. *Nature Climate Change* 2: 417-424.Briffa KR, Shishov VV, Melvin TM, et al. (2008) Trends in recent temperature and radial tree growth spanning 2000 years across northwest Eurasia. *Philosophical Transactions of the Royal Society B-Biological Sciences* 363: 2271-2284.

Brohan P, Kennedy JJ, Harris I, et al. (2006) Uncertainty estimates in regional and global observed temperature changes: A new data set from 1850. *Journal of Geophysical Research-Atmospheres* 111: 21.

Cook ER, Briffa KR, Meko DM, et al. (1995) The segment length curse in long tree-ring chronology development for palaeoclimatic studies. *Holocene* 5: 229-237.

Craig H. (1961) Isotopic variations in meteoric waters. *Science* 133: 1702-1703.

Dansgaard W. (1964) Stable isotopes in precipitation. *Tellus* 16: 436-468.

Dewald A, Heinze S, Jolie J, et al. (2013) CologneAMS, a dedicated center for accelerator mass spectrometry in Germany. *Nuclear Instruments & Methods in Physics Research Section B-Beam Interactions with Materials and Atoms* 294: 18-23.

Faber A-K, Vinter BM, Sjolte J, et al. (2016) How does sea ice influence $\delta^{18}O$ of Arctic precipitation? *Atmospheric Chemistry and Physics Discussions* in review.

Grootes PM, Nadeau MJ and Rieck A. (2004) C-14-AMS at the Leibniz-Labor: radiometric dating and isotope research. *Nuclear Instruments & Methods in Physics Research Section B-Beam Interactions with Materials and Atoms* 223: 55-61.

Günther F, Overduin PP, Sandakov AV, et al. (2013) Short- and long-term thermo-erosion of ice-rich permafrost coasts in the Laptev Sea region. *Biogeosciences* 10: 4297-4318.

Hughes MK, Vaganov EA, Shiyatov S, et al. (1999) Twentieth-century summer warmth in northern Yakutia in a 600-year context. *Holocene* 9: 629-634.

Joos F and Spahni R. (2008) Rates of change in natural and anthropogenic radiative forcing over the past 20,000 years. *Proceedings of the National Academy of Sciences of the United States of America* 105: 1425-1430.

Kaufman DS, Schneider DP, McKay NP, et al. (2009) Recent Warming Reverses Long-Term Arctic Cooling. *Science* 325: 1236-1239.

Lachenbruch AH. (1962) Mechanics of Thermal Contraction Cracks and Ice-Wedge Polygons in Permafrost. *Geological Society of America Special Papers* 70: 1-66.

Laskar J, Robutel P, Joutel F, et al. (2004) A long-term numerical solution for the insolation quantities of the Earth. *Astronomy & Astrophysics* 428: 261-285.

Liu Z, Zhu J, Rosenthal Y, et al. (2014) The Holocene temperature conundrum. *Proceedings of the National Academy of Sciences of the United States of America* 111: E3501-E3505.

MacDonald GM, Case RA and Szeicz JM. (1998) A 538-year record of climate and treeline dynamics from the lower Lena River region of northern Siberia, Russia. *Arctic and Alpine Research* 30: 334-339.

Mackay JR. (1983) Oxygen isotope variations in permafrost, Tuktoyaktuk Peninsula area, Northwest Territories. *Current Research, Part B, Geological Survey of Canada* Paper 83-1B: 67-74.

McKay NP and Kaufman DS. (2014) An extended Arctic proxy temperature database for the past 2,000 years. *Scientific Data* 1.

Merlivat L and Jouzel J. (1979) Global Climatic Interpretation of the Deuterium-Oxygen 18 Relationship for Precipitation. *Journal of Geophysical Research-Oceans and Atmospheres* 84: 5029-5033.

Meyer H, Dereviagin AY, Siegert C, et al. (2002a) Paleoclimate studies on Bykovsky Peninsula, North Siberia-hydrogen and oxygen isotopes in ground ice. *Polarforschung* 70: 37-51.

Meyer H, Dereviagin AY, Siegert C, et al. (2002b) Palaeoclimate reconstruction on Big Lyakhovsky Island, North Siberia - Hydrogen and oxygen isotopes in ice wedges. *Permafrost and Periglacial Processes* 13: 91-105.

Meyer H, Opel T, Laepple T, et al. (2015) Long-term winter warming trend in the Siberian Arctic during the mid-to late Holocene. *Nature Geoscience* 8: 122-125.

Meyer H, Schirrmeister L, Yoshikawa K, et al. (2010) Permafrost evidence for severe winter cooling during the Younger Dryas in northern Alaska. *Geophysical Research Letters* 37: L03501.

Meyer H, Schönicke L, Wand U, et al. (2000) Isotope studies of hydrogen and oxygen in ground ice - Experiences with the equilibration technique. *Isotopes in Environmental and Health Studies* 36: 133-149.

Opel T, Dereviagin AY, Meyer H, et al. (2011) Palaeoclimatic Information from Stable Water Isotopes of Holocene Ice Wedges on the Dmitrii Laptev Strait, Northeast Siberia, Russia. *Permafrost and Periglacial Processes* 22: 84-100.

Opel T, Fritzsche D and Meyer H. (2013) Eurasian Arctic climate over the past millennium as recorded in the Akademii Nauk ice core (Severnaya Zemlya). *Climate of the Past* 9: 2379-2389.

Opel T, Wetterich S, Meyer H, et al. (2017) Ground-ice stable isotopes and cryostratigraphy reflect late Quaternary palaeoclimate in the Northeast Siberian Arctic (Oyogos Yar coast, Dmitry Laptev Strait). *Climate of the Past Discussions*: 1-37.PAGES 2k Consortium. (2013) Continental-scale temperature variability during the past two millennia. *Nature Geoscience* 6: 339-346.

Reimer PJ, Bard E, Bayliss A, et al. (2013) IntCal13 and Marine13 Radiocarbon Age Calibration Curves 0–50,000 Years cal BP. *Radiocarbon* 55: 1869-1887.

Reimer PJ, Brown TA and Reimer RW. (2004) Discussion: Reporting and calibration of post-bomb C-14 data. *Radiocarbon* 46: 1299-1304.

Rethemeyer J, Fulop RH, Hofle S, et al. (2013) Status report on sample preparation facilities for C-14 analysis at the new CologneAMS center. *Nuclear Instruments & Methods in Physics Research Section B-Beam Interactions with Materials and Atoms* 294: 168-172.

Schirrmeister L, Kunitsky V, Grosse G, et al. (2011) Sedimentary characteristics and origin of the Late Pleistocene Ice Complex on north-east Siberian Arctic coastal lowlands and islands - A review. *Quaternary International* 241: 3-25.

Screen JA and Simmonds I. (2010) The central role of diminishing sea ice in recent Arctic temperature amplification. *Nature* 464: 1334-1337.

Serreze MC and Barry RG. (2011) Processes and impacts of Arctic amplification: A research synthesis. *Global and Planetary Change* 77: 85-96.

Streletskaya ID, Vasiliev AA, Oblogov GE, et al. (2015) Reconstruction of paleoclimate of Russian Arctic in the Late Pleistocene–Holocene on the basis of isotope study of ice wedges. *Kriosfera Zemli* 19: 86-94.

Stuiver M and Polach HA. (1977) Reporting of 14C Data - Discussion. *Radiocarbon* 19: 355-363.

Sundqvist HS, Kaufman DS, McKay NP, et al. (2014) Arctic Holocene proxy climate database – new approaches to assessing geochronological accuracy and encoding climate variables. *Climate of the Past* 10: 1605-1631.Taylor KE, Stouffer RJ and Meehl GA. (2012) An Overview of CMIP5 and the Experiment Design. *Bulletin of the American Meteorological Society* 93: 485-498.

Vaikmäe R. (1989) Oxygen isotopes in permafrost and ground ice: A new tool for paleoclimatic investigations. *5th Working Meeting Isotopes in Nature, Leipzig, September 1989, Proceedings.* 543-553.

Vasil'chuk Y and Vasil'chuk A. (2014) Spatial distribution of mean winter air temperatures in Siberian permafrost at 20-18ka BP using oxygen isotope data. *Boreas* 43: 678-687.

Vasil'chuk YK, Budantseva NA, Christiansen HH, et al. (2015) Oxygen stable isotope variation in Late Holocene ice wedges in Yamal Peninsula and Svalbard. *Geography, Environment, Sustainability* 8: 36-54.

Werner M, Langebroek PM, Carlsen T, et al. (2011) Stable water isotopes in the ECHAM5 general circulation model: Toward high-resolution isotope modeling on a global scale. *Journal of Geophysical Research-Atmospheres* 116: 14.

Wetterich S, Rudaya N, Tumskoy V, et al. (2011) Last Glacial Maximum records in permafrost of the East Siberian Arctic. *Quaternary Science Reviews* 30: 3139-3151.

Wetterich S, Schirrmeister L, Andreev AA, et al. (2009) Eemian and Late Glacial/Holocene palaeoenvironmental records from permafrost sequences at the Dmitry Laptev Strait (NE Siberia, Russia). *Palaeogeography Palaeoclimatology Palaeoecology* 279: 73-95.

Wetterich S, Tumskoy V, Rudaya N, et al. (2014) Ice Complex formation in arctic East Siberia during the MIS3 Interstadial. *Quaternary Science Reviews* 84: 39-55.

Wetterich S, Tumskoy V, Rudaya N, et al. (2016) Ice Complex permafrost of MIS5 age in the Dmitry Laptev Strait coastal region (East Siberian Arctic). *Quaternary Science Reviews*.

Zhang Q, Sundqvist HS, Moberg A, et al. (2010) Climate change between the mid and late Holocene in northern high latitudes - Part 2: Model-data comparisons. *Climate of the Past* 6: 609-626.

Tables and Figures

Table 1: Radiocarbon ages of organic remains in Oyogos Yar ice-wedge samples and corresponding $\delta^{18}O$ values. The excluded radiocarbon ages are given in brackets. The sample marked by the asterisk was calibrated with CaliBomb. Additionally the mean $\delta^{18}O$ value of RIW is presented.

Sample ID	Lab ID	Radiocarbon age [yr BP]	Calibrated age midpoint of hdp [yr cal AD]	Range of hpd [± yr]	Probability [%]	$\delta^{18}O$ [‰; V-SMOW]
RIW	-	-	2003.5	3.5	-	-20.7
Ice wedge Oy7-04 IW2						
Oy7-04-205	COL 3997	1607 ± 49 BP	451	112	95	-25,5
Oy7-04-242	KIA 35630	523 ± 46 BP	1417	31	66.6	-25.9
Oy7-04-247	KIA 35631	(3518 ± 31 BP)	-1838	86.5	95	-22.8
Oy7-04-263	KIA 35632	412 ± 30 BP	1474	43.5	84	-22.7
Oy7-04-267	KIA 35633	258 ± 51 BP	1544	60	37.2	-25.0
Oy7-04-274	KIA 35634	488 ± 58 BP	1448	64.5	76.9	-25.8
Oy7-04-290	KIA 35635	1479 ± 106 BP	547	171	91.6	-25.9
Ice wedge Oy7-11 IW2						
Oy7-11-138	KIA 35636	(8959 ± 43 BP)	-8221	55	49	-26.6
Oy7-11-162	KIA 35637	(8300 ± 43 BP)	-7365	119	86.6	-25.5
Oy7-11-189	KIA 35638	857 ± 47 BP	1204	58	69.3	-23.0
Ice wedge Oy7-11 IW7						
Oy7-11-719	KIA 40385	1858 ± 60 BP	152	106.5	87	-25.9
Oy7-11-723	KIA 40386	1868 ± 36 BP	152	81	95	-24.9
Oy7-11-740	KIA 40387	1081 ± 22 BP	978	36.5	68.9	-24.8
Oy7-11-747	KIA 40388	1098 ± 24 BP	942	50.5	95	-25.4
Oy7-11-796*	KIA 40390	$F^{14}C$ 1.2661 ±	1981	1	84.0	-21.9

		0.005				
Oy7-11-820	KIA 40391	225 ± 25 BP	1661	19	43.6	-24.4
Oy7-11-Hy27	COL 1925	1579 ± 43 BP	482	86.5	95	-23.9
Oy7-11-Hy31	KIA 40393	(14200 ± 71 BP)	-15342	227.5	95	-25.3
Oy7-11-Hy40	KIA 40394	(6640 ± 51 BP)	-5560	73.5	95	-25.3

1

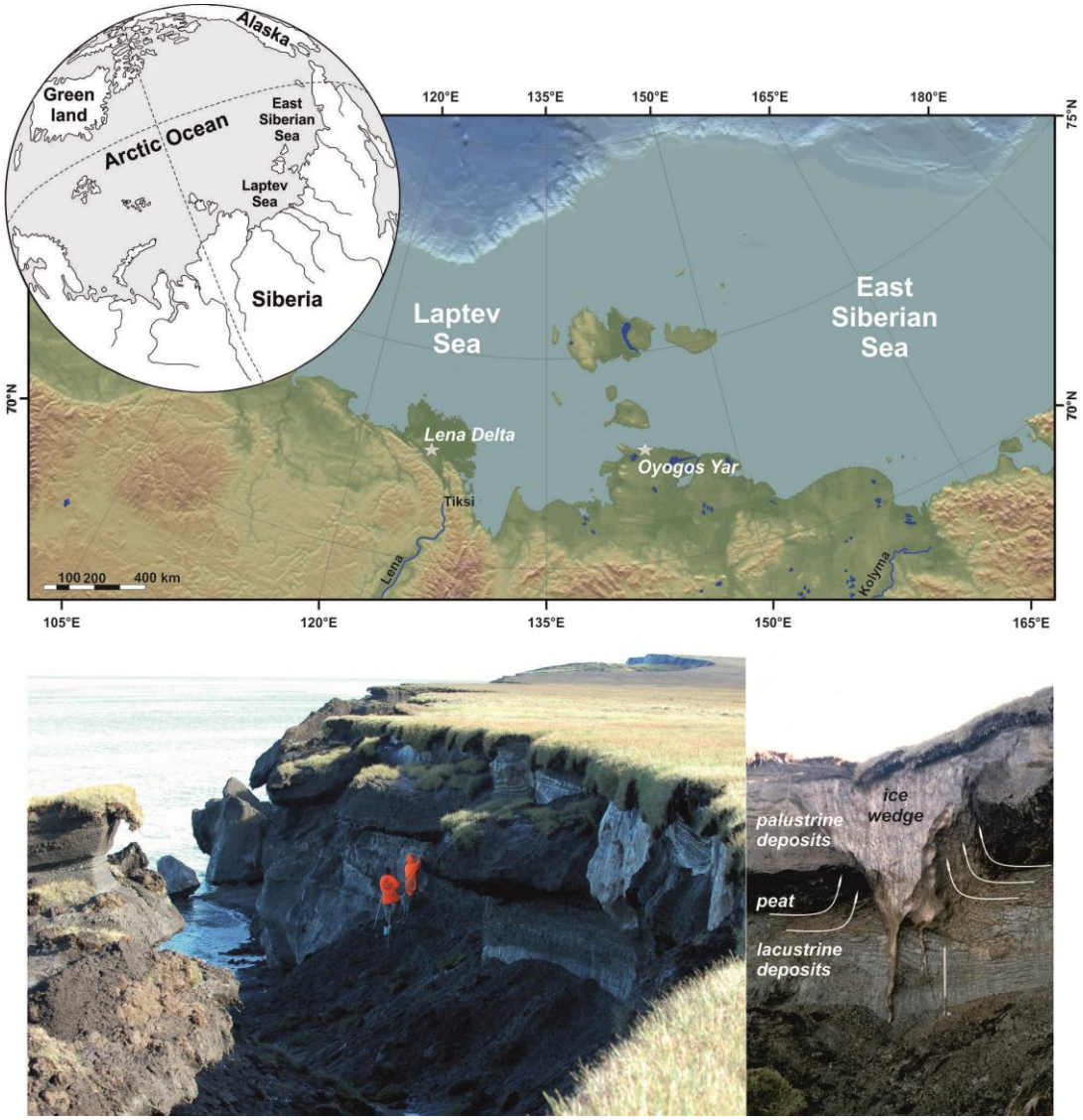

Figure 1: Location map of the study region and photographs of the stratigraphy and ice wedges.

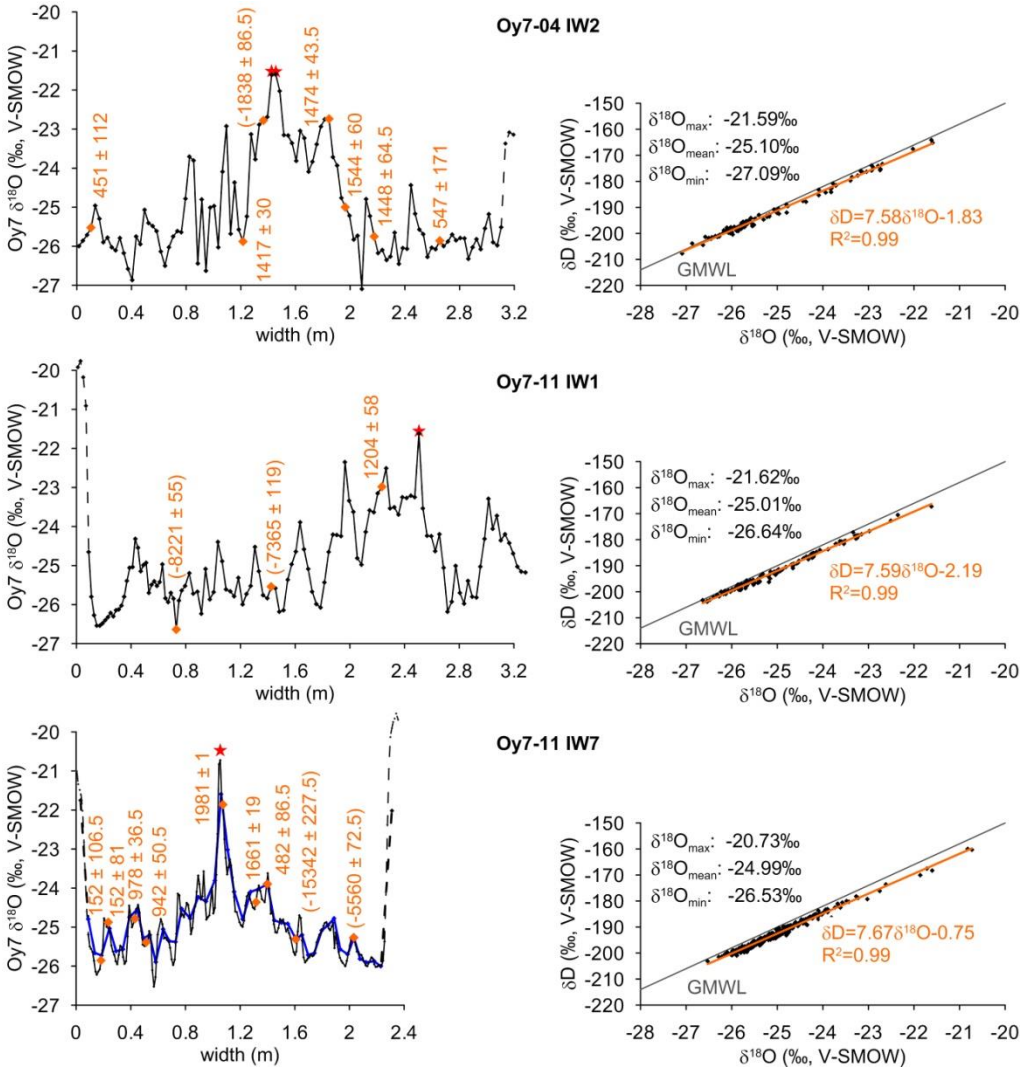

Figure 2: Ice-wedge $\delta^{18}O$ profiles with calibrated radiocarbon ages (years AD) and $\delta^{18}O$-δD co-isotopic plots for the three studied ice wedges from Oyogos Yar. Grey dots and lines as well as ages in brackets in the profiles refer to excluded marginal samples and excluded ages. Red stars represent the recent growth stages of ice wedges. For Oy7-11-IW7 the thick blue line refers to the low-resolution profile.

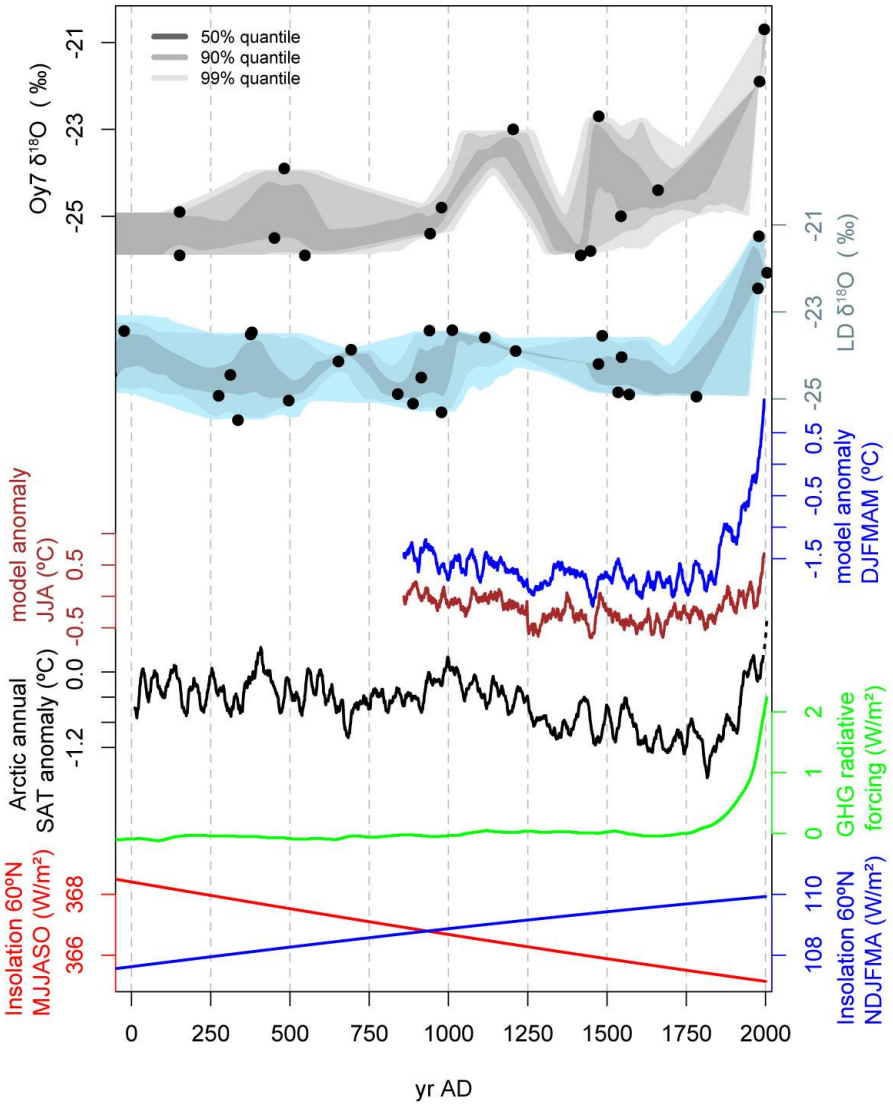

1

2 Figure 3: Oyogos Yar (Oy7) ice-wedge $\delta^{18}O$ stack compared to Lena River Delta (LD)
3 ice-wedge $\delta^{18}O$ stack, modelled surface air temperatures for the study region (20-year
4 running mean, anomalies relative to AD1961-1990), Arctic annual temperature

anomalies (20-year running mean, anomalies relative to AD1961-1990) reconstructed (line) (McKay and Kaufman, 2014) and 60-90°N HadCRUT3 instrumental (dotted) (Brohan et al., 2006), greenhouse gas (GHG) forcing (Joos and Spahni, 2008) and seasonal insolation forcing (Laskar et al., 2004). The grey bands show the uncertainty caused by the radiocarbon dating, and the black dots show the $\delta^{18}O$ values at the midpoint of the age distribution.